Bulletin of the
Chemical
Society of
Japan

Nano-silica@PVC-Bonded N-Ethyl Sulfamic Acid as a Recyclable Solid Catalyst for the Hydroxyalkylation of Phenol with Formaldehyde to Bisphenol F

Dabo Jiang, Shuolin Zhou, Zaihui Fu,* Qiong Xu, Jiafu Xiao, Min Zheng, Wenzhou Zhong,
Xianxiang Liu, Steven Robert Kirk, and Dulin Yin*

Advance Publication on the web June 1, 2019
doi:10.1246/bcsj.20190081

Nano-silica@PVC-Bonded N-Ethyl Sulfamic Acid as a Recyclable Solid Catalyst for the Hydroxyalkylation of Phenol with Formaldehyde to Bisphenol F

Dabo Jiang,[1] Shuolin Zhou,[1,2] Zaihui Fu,*[1] Qiong Xu,[1] Jiafu Xiao,[1] Min Zheng,[1,3] Wenzhou Zhong,[1] Xianxiang Liu,[1] Steven Robert Kirk,[1] and Dulin Yin*[1]

[1] National & Local Joint Engineering Laboratory for New Petro-chemical Materials and Fine Utilization of Resources, College of Chemistry and Chemical Engineering, Hunan Normal University Changsha 410081 (China).

[2] Educational Scientific Institute, Changsha Normal University, Changsha Hunan 410100 (China)

[3] Educational Scientific Institute, Hunan First Normal University, Changsha Hunan 410205 (China)

E-mail: < fzhhnnu@126.com, dulinyin@126.com>

Zai hui Fu

Zai hui Fu, is a professor at the Institute of Fine Catalytic Synthesis, Hunan Normal University. His research interests involve molecular design of new catalytic materials, green catalytic oxidation and enzyme-like catalytic conversion. Related research achievements are published in many domestic and foreign academic journals.

Abstract

Sulfamic acid functionalized PVC-coated nano-silica (NS) catalyst (NS@PVC-EDA-SO_3H) was prepared *via* multi-steps treatment processes and characterized by FT-IR, N_2 adsorption-desorption, TGA/DTG, XRD, TEM, STEM-EDS, as well as acid-base back-titration. The hydroxyalkylation of phenol with formaldehyde to bisphenol F was employed to in details evaluate its acid catalysis performances. The results indicated that the newly constructed NS@PVC-EDA-SO_3H possessed richer short mesoporous to macroporous channels and highly exposed sulfamic acids and could exhibit excellent hydroxyalkylation activity and reusability owing to it's fast mass transfer and reaction rates for the conversion of substrates, as well as its excellent structural and chemical stabilities. This new solid acid was obviously superior to the conventional homogeneous concentrated sulfuric acid and heterogeneous sulfonated resin catalysts in catalytic activity and reusability, which could achieve a remarkable formaldehyde conversion (99.9%) and selectivity of bisphenol F (94.5%) under optimal hydroxyalkylation. conditions. Furthermore, it could also be recovered easily and used repeatedly at least nine times without an obvious decrease in activity.

Keywords: Solid acid catalyst, Sulfamic Acid, Hydroxyalkylation

1. Introduction

The synthesis of bisphenol F (BPF) has been given extensive attention due to the increasing demand and applicability in plastics, resins and rubber industries[1,2]. Conventionally, the method for the preparation of BPF is based on the condensation reaction of phenol and formaldehyde using a liquid protonic acid such as phosphoric acid, hydrochloric acid, sulfuric acid or other inorganic acids etc. as catalyst, owing to their high activity and low cost[3-6]. These homogeneous catalysis systems, however, suffer from several drawbacks such as high toxicity, hazards of handling, corrosion of equipment and difficulty in separation and recovery [7, 8]. It is, therefore, of great practical importance to develop easily separable and reusable solid catalysts having high activity for the synthesis of BPF. Recently, a series of works have been reported to replace the conventional liquid protonic acids by solid acid catalysts, such as heteropolyacid catalysts[9], acid functionalized molecular sieves[10], clay[11] and H-beta zeolite [12]. Phosphotungstic acid encapsulated in metal-organic frameworks PTA@MIL-100 (Fe or Cr) (β) was also reported as an efficient solid catalyst for synthesis of BPF by Chen et. al. and showed high yield (92.1%) and selectivity (93.0%) for the hydroxyalkylation of phenol with formaldehyde to BPF. Unfortunately, not only are the synthesis routes of these catalysts complex, but their stability is also poor[13]. An aluminum-grafted MCM-41 molecular sieve used as a catalyst, also having higher yield (93.2%) and selectivity (91.1%) for the reaction, was reported by Suman K. J et. al.[14], who suggested that these catalysts possess high surface areas which can accelerate the progress of the reaction. The reaction conditions, however (phenol/formaldehyde up to 30 mol·mol^{-1}, catalyst concentration of 15 wt.%, reaction temperature of 90 and reaction time of 4 h), were relatively harsh in terms of energy consumption for the industrial BPF process, and no evidence was provided for the reuse and stability of the catalysts. Short-channeled mesoporous Zr-Al-SBA-15, as an efficient catalyst for hydroxyalkylation of phenol with formaldehyde, was reported by Wei et. al:[15] in this case, a maximum BPF yield of 96.1% was obtained. But the reusability of these catalysts is poor: the catalyst can only be recycled four times, with an accompanying marked decline in catalytic performance. The use of DTP ($H_3PW_{12}O_{40}$)-impregnated fumed silica (DTP/SiO_2) as an effective catalyst for the reaction was reported by Garade et. al.[16], giving a higher selectivity (90.1%) to BPF. But the low yield (34.2%) and poor reusability (two times) severely restricted its application for the hydroxyalkylation of phenol with formaldehyde to BPF.

Herein, relying critically on the fulfillment of certain green chemistry principles such as the ease-inexpensiveness, environmental friendliness, high efficiency, we report an efficient method for the preparation of NS-coated PVC bearing sulfamic acid (NS@PVC-EDA-SO_3H) as a stable and robust heterogeneous catalyst for the hydroxyalkylation of phenol with formaldehyde to BPF. As shown in scheme 1, NS-coated PVC material (NS@PVC) was prepared via a simple impregnation method; And then the sulfonation sites were introduced on NS@PVC by N-alkylation of ethylenediamine with PVC, yielding the EDA grafted NS@PVC material (NS@PVC-EDA) and the latter was finally converted to the

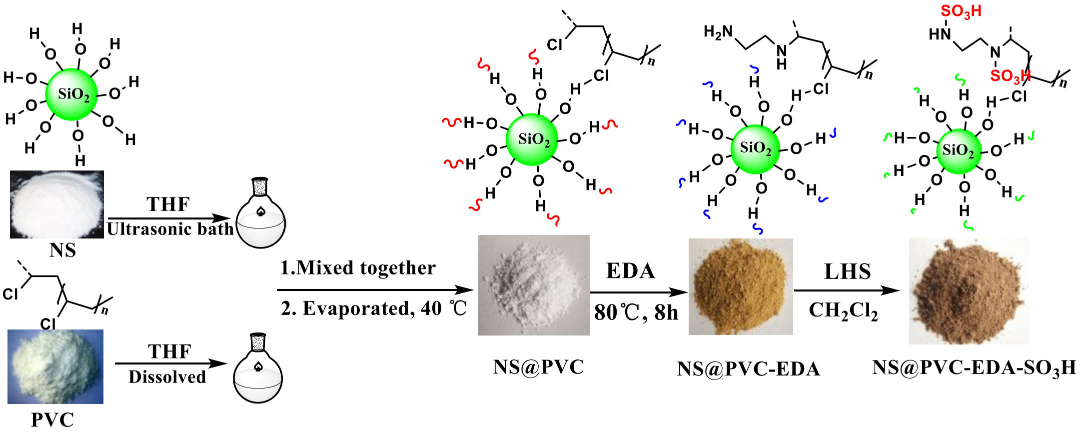

Scheme 1. Synthetic routes to NS@PVC-EDA-SO_3H catalyst with inset corresponding photograph.

goal catalyst through grafting chlorosulfonic acid (LHS). Series of characterizations have confirmed that the newly constructed solid acid has richer short mesoporous to macroporous channels and highly exposed and stable sulfamic acids and can remarkably accelerate the diffusion and conversion of substrates on it[17-20], thus showing excellent hydroxyalkylation activity and reusability in the synthesis of BPF.

2. Experimental

2.1 Materials: Polyvinyl chloride (polymerization degree 1580~1780, PVC), Silicon dioxide (99.5%, 20±5 nm), Tetrahydrofuran (≥99.0%, THF), ethanol (≥99.0%), ethylenediamine (≥99.0%, EDA), dichloromethane (≥99.5%), phenol (≥99.0%), formaldehyde solution (38.2%) were purchased from Sinopharm Chemical Reagent Co., Ltd; (Shanghai, China) and used without further purification. Methanol was purchased from TEDIA (HPLC grade, USA). Chlorosulfonic acid (≥99.0%, LHS) was purchased from Xiya Chemical Co., Ltd (Chengdu, China). Water used in the laboratory was prepared by a Millipore Milli-Q ultrapure water-purification system.

2.2 Preparation of the catalyst:

NS@PVC: For the preparation of NS@PVC, the phase inversion method was used [21]. The activated NS powder of 10 g was added to 100 mL of tetrahydrofuran (THF) solution and then dispersed to form a stable suspension solution under an ultrasound treatment for 30 min. The obtained suspension solution was mixed with 4 g PVC dissolved in 100 mL THF and then stirred at room temperature for 24 h. Finally, this mixed solution was evaporated to obtain NS@ PVC material at 40°C.

NS@PVC-EDA: 5 g NS@PVC was mixed with an excess of ethylenediamine (40 mL) in a reaction vessel equipped with a condenser. The resulting mixture was refluxed at 80°C for 8 h under stirring. The reaction mixture was then cooled to room temperature and filtered through a vacuum glass filter. The filter-cake was washed sequentially with a large excess of ethanol and dried under vacuum overnight at 60°C to give the desired product NS@PVC-EDA, as a yellow powder.

NS@PVC-EDA-SO_3H: Referring to the preparation of $CoFe_2O_4$ nanoparticle immobilized N-propyl diethylenetriamine sulfamic acid catalyst [22], chlorosulfonic acid (10 ml) was added dropwise to a magnetically stirred mixture of NS@PVC-EDA (2.5 g) in CH_2Cl_2 (20 ml) at 0°C over a period of 2 h. Upon completion of the reaction, the mixture was stirred for 24 h and then filtered. The filter-cake was washed with a large excess of ethanol and dried under vacuum overnight at 60°C to afford the desired product, NS@PVC-EDA-SO_3H, as a brown powder.

2.3 Catalytic performance tests: The hydroxyalkylation of phenol with formaldehyde to BPF was performed in a magnetically stirred glass reactor fitted with a reflux condenser and an arrangement for temperature control. In a typical procedure, 0.2 mol of phenol, 0.01 mol of formaldehyde and catalyst (0.02 g, 0.25 mol%, based on the acid density of the catalyst) were added into the reactor. No other solvent was needed. The reaction mixture was heated to 70°C. After 1 h, the reaction was stopped and cooled down to room temperature, then the solid catalysts were separated by filtration, washed with aqueous ethanol, and then was dried overnight at 60°C in a vacuum drying oven for reuse.
The unreacted formaldehyde was determined using an UV-2450 spectrophotometer (Shimadzu, Kyoto, Japan) using an acetylacetone spectrophotometric method [23,24]. The compositions of the hydroxyalkylated products were determined on an Agilent 1100 HPLC (Agilent, USA) with an external standard method[14,15] and the specific operation conditions were as follows: 4.6×250 mm of Agilent SB-C 18 chromatographic column, methanol/water 65:35 (v/v) of mobile phase, 1.0 ml/min of flow rate, the UV detector 270 nm, column temperature 30°C, injection volume 20 μL. The activity of catalyst was evaluated in terms of formaldehyde conversion and the selectivity of bisphenols F, which were calculated as follows:

$$\text{Conversion (\%)} = \frac{\text{moles of reacted formaldehyde}}{\text{moles of formaldehyde}} \times 100\%$$

$$\text{Selectivity (\%)} = \frac{\text{moles of bisphenols F}}{\sum \text{moles of all products}} \times 100\%$$

2.4 Characterization of catalyst: X-ray diffraction spectroscopy (XRD) was performed with a Bruker D8-Advance X-ray diffractometer, under the following conditions: Cu target K αray (λ=1.54187 Å); scanning voltage 40 kV, scanning current 40 mA; scanning speed 0.2 s, scanning step 0.02 °. The materials were identified using the ICDD/JCPDS database. FT-IR spectra of the samples were tested by the KBr pellet technique on a Nicolet Avata 370 Fourier-transform infrared spectrophotometer in the range 400~4000 cm^{-1}. N_2 adsorption-desorption isotherms were recorded with an ASAP 2400 physisorption instrument made by Micromeritics Corporation (UNITED STATES). Prior to measurement, all samples were dried under vacuum at 60°C for 24 h. The specific surface area was calculated by BET method. Pore size distribution was calculated by BJH method. Thermogravimetric analyses (TG) were performed with a NETZSCH-STA 409 PC thermoanalyzer at a heating rate of 10°C/min under oxygen atmosphere. The morphology of the NS@PVC-EDA-SO_3H

catalyst was determined using High-resolution transmission electron microscopy (HR-TEM; JEM 2100, JEOL, Japan). The EDS was measured using a JEOL JSM-2000EM scanning electron microscope. Referring to the literature[25], The measurement for the -SO_3H groups of catalyst was described as follows: a catalyst (0.05 g) was treated with 0.005 mol·L^{-1} of NaOH solution (20 mL) for 1 h at 20~50°C under ultrasonic vibration. After the removal of catalyst, the resulting filtrate was titrated with 0.005 mol·L^{-1} of HCl solution. The acid density was calculated as follows:

$$Q_e = \frac{V_{(NaOH)}c_{(NaOH)} - V_{(HCl)}c_{(HCl)}}{w}$$

Where $c_{(NaOH)}$ and $c_{(HCl)}$ are the concentrations of the standard aqueous NaOH and HCl solution, respectively. $V_{(HCl)}$ is the volume (mL) of the standard aqueous HCl used in the titration, $V_{(NaOH)}$ is the volume (mL) of the standard aqueous NaOH solution (20 mL), and w is the sample weight (g), Q_e is the acid density of catalyst.

3. Results and Discussion

3.1 Characterization:

FT-IR: Figure 1 gives the FT-IR spectra of NS@PVC-EDA-SO_3H and its precursors. The FT-IR spectrum of PVC shows its some characteristic peaks, including two peaks at 2912 and 1429 cm^{-1} respectively attributed to the stretching and wagging vibrations of C-H from CH_2 groups, three peaks at 2968, 1331 and 1254 cm^{-1} respectively originating from the stretching and deformation of C-H of CHCl groups, as well as two peaks at 690 cm^{-1} and 613 cm^{-1}assigned to C-Cl bond stretching[26,27]. The FT-IR spectrum of NS exhibits two peaks at 798 and 1110 cm^{-1}, which are initiated by Si-O-Si symmetric and asymmetric stretching vibrations, respectively. NS@PVC also shows the above characteristic peaks belonged to PVC and NS in its FT-IR spectrum, supporting that this material is composed of PVC and NS. Comparing with NS@PVC, NS@PVC-EDA shows a new peak at 1652 cm^{-1} due to the bending vibration of N-H bond and a disappearance of the C-Cl peak at 615 cm^{-1} is found in its FT-IR spectrum, and the peak at 3420 cm^{-1} is larger than NS@PVC, perhaps because the graft of the N-H bond results in the absorption peak being stronger after N-alkylation, indicating that EDA is successfully grafted on the carbon chain of PVC loaded NS *via* N-alkylation. The FT-IR spectrum of NS@PVC-EDA-SO_3H shows the peak at about 1110 cm^{-1} is attributed to the typical symmetric stretching vibration of Si–O–Si and the vibration bands of SO_3^- stretching of supported SO_3H group. However, the peak cannot be resolved due to its overlap with the absorbance of Si–O–Si stretch in the 970–1310 cm^{-1}. And the peak at 1380 cm^{-1} may be attributed to the O=S=O stretching band of sulfamic group, whereas the N–S stretch was present at 691 cm^{-1}, confirming the successful grafting of chlorosulfonic acids on NS@PVC-EDA [28-31].

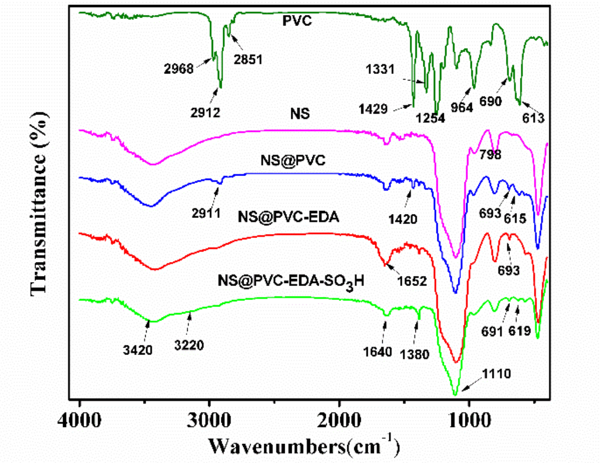

Figure 1. FT-IR spectra of NS, PVC, NS@PVC, NS@PVC-EDA, NS@PVC-EDA-SO_3H samples.

N_2 adsorption-desorption: Figure 2 is the physical adsorption-desorption isotherms of N_2 at -196°C and pore size distributions for the above samples and the calculated porous parameters including the BET surface area, pore volume and BJH pore size are listed Table 1. As shown in Figure 2(a), the raw material PVC presents a typical non-porous feature in its adsorption-desorption isotherms. While NS support exhibits typical type III adsorption-desorption isotherms with a BET surface area of 147 m^2•g^{-1} and a porous volume of 1.08 cm^3•g^{-1}, its BJH curve presents a broad pore size distribution from 10 to 100 nm, indicating that NS, NS@PVC, NS@PVC-EDA, NS@PVC-EDA-SO_3H samples contains richer mesoporous to microporous channels, whereas the observed pores (Figure 2b) are mostly due to the gap between those particles. In addition, the materials that NS is combined with PVC and its functionalized derivatives also show a similar III adsorption-desorption isotherm and BJH pore size distribution to pure NS (Figure 2b), but their BET surface areas and pore volumes decrease to some extent, along with an increase of their average pore sizes. Moreover, the change of these porous parameters is becoming more and more prominent with the continuous functionalization of PVC by successively grafting EDA and LHS (Table 1). This supports that the impregnation of PVC partly occurs in the macropores and especially mesopores of NS and its further functionalization can remarkably increase its ratio to enter the pores of NS.

Table 1. The specific surface areas (S_{BET}), pore volume (Vg) and average pore size (D) of PVC, NS, NS@PVC, NS@PVC-EDA, NS@PVC- EDA-SO_3H.

Samples	S_{BET} (m^2/g)	Vg (cm^3/g)	D (nm)
PVC	3	0.01	22
NS (support)	147	1.08	36
NS@PVC	123	1.13	39
NS@PVC-EDA	88	1.08	44
NS@PVC-EDA-SO_3H	48	0.57	50

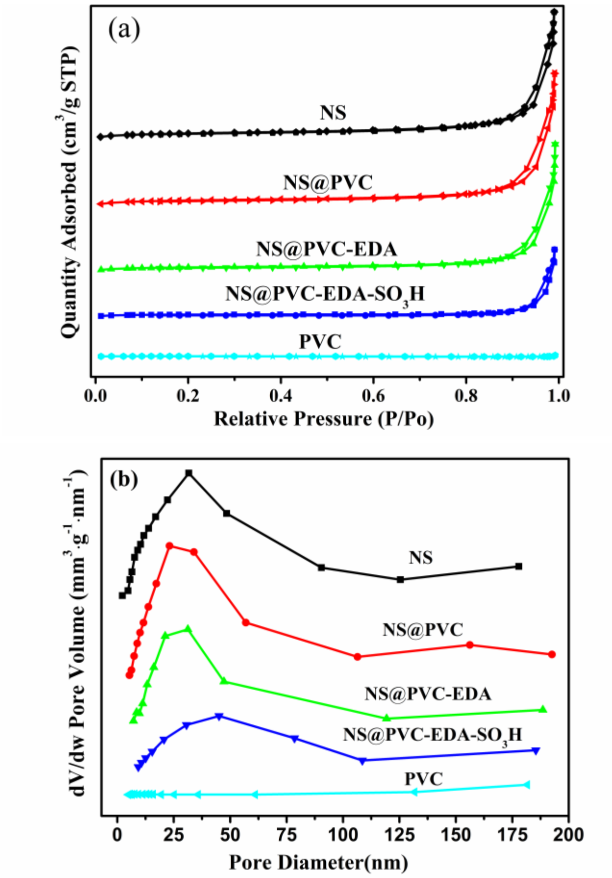

Figure 2. N_2 adsorption-desorption isotherms and pore size distributions of PVC, NS, NS@PVC, NS@PVC-EDA, NS@PVC-EDA-SO_3H samples.

TG/DTG: The thermal decomposition behavior of the above samples under oxygen atmosphere was investigated by a thermal gravimetric analysis (TGA) technique and the obtained TG and differential TG (DTG) curves are shown in Figure 3. It is seen from the TG and DTG curves of two raw materials that NS support itself has no obvious weight loss process during the temperature range examined, indicating its high thermal stability. While pure PVC shows two significant weight loss peaks at 298 and 511°C in its DTG curve, respectively corresponding to the dehydrochlorination of PVC and the further oxidation degradation of its dehydrochlorinated residues[32-34]. When PVC was loaded on NS, its two weight loss peaks can still be found in the DTG curve of NS@PVC sample although they are weakened remarkably in intensity. And the estimated PVC loading from the TG curve of NS@PVC is about 22.8%. From the TG and DTG curves of NS@PVC-EDA, it can be seen that the weight loss attributable to the dehydrochlorination of PVC is weakened after PVC grafting EDA. In addition, a new weight loss occurs about 100ºC, which is likely due to the evaporation of the adsorbed water. These findings indicate that most C-Cl bonds of PVC have been successfully substituted by C-N bonds via N-alkylation and such substitution can increase hydrophilicity of NS@PVC-EDA. After NS@PVC-EDA further grafting LHS, its weight loss peak for the adsorbed water is slightly strengthened owing to the grafting of polar LHS. In addition, a weight loss between 150-400ºC could be assigned to removal of organic motif (ethylenediamine and sulfamic acid) from the structure of NS@PVC-EDA-SO_3H [35].

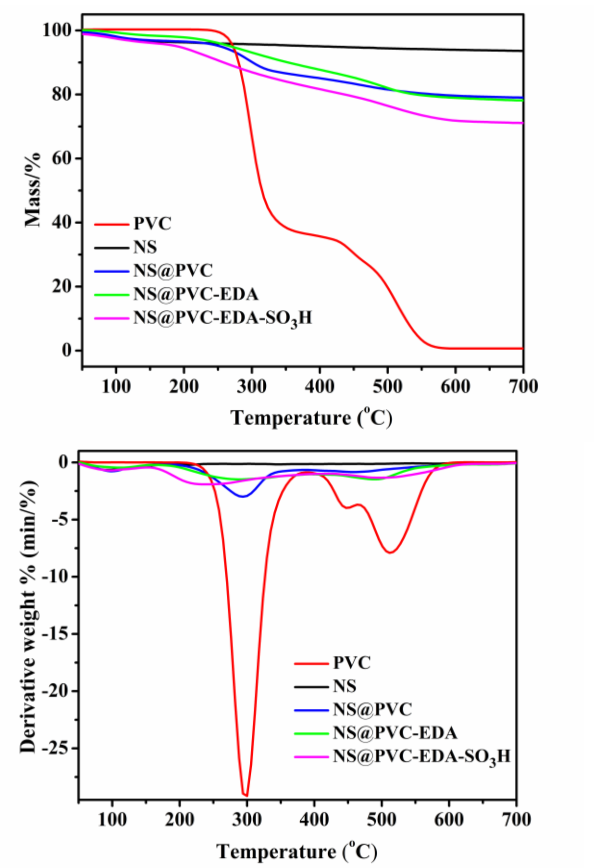

Figure 3. TG thermograms and derivative thermogravimetric (DTG) curves of PVC, NS, NS@PVC, NS@PVC-EDA, NS@PVC-EDA-SO_3H samples.

XRD: Powder X-ray diffraction (XRD) spectra of these samples are shown in Figure 4. An amorphous structure character of NS support is clearly observable in its XRD spectrum, consistent with previous reports[36,37]. The amorphous structure of PVC is also indicated by the broad peak appearing in the region of 15~30º. In addition, the XRD spectra of NS@PVC, NS@PVC-EDA, NS@PVC-EDA-SO_3H samples are very similar to that of NS, which suggests an amorphous structure for these samples.

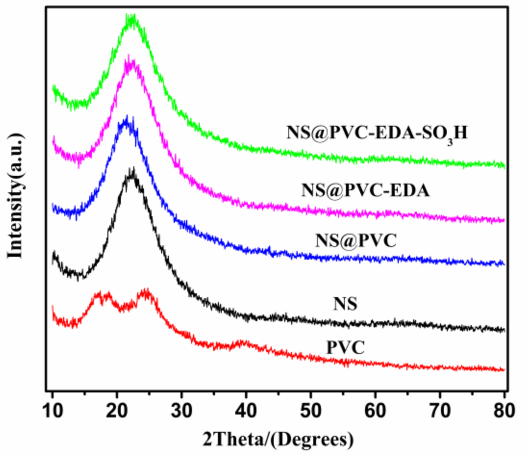

Figure 4. XRD pattern for PVC, NS, NS@PVC, NS@PVC-EDA, NS@PVC-EDA-SO_3H samples.

TEM: The morphology of NS@PVC-EDA-SO_3H catalyst was characterized by high resolution transmission electron microscopy (HRTEM) and its three HRTEM micrograph are given in Figure 5. Figure 5(c, d) demonstrates that NS has an average diameter of 15–20 nm, however most of the NS particles have an agglomerated appearance. This catalyst presents an irregular spherical structure in morphology and most of its nanoparticles are located in 20 to 30 nm (Figure 5a, b). In addition, the PVC film coated on the surface of NS can also be clearly discerned from its high resolution HRTEM images and the thickness of this coated film is estimated to be 5–10 nm. By the way, some the naked NS particles and uncoated PVC films, which are marked in the red and green regions, respectively, are also found in its HRTEM images, indicating that at least a portion of the PVC derivative is not coated on the NS.

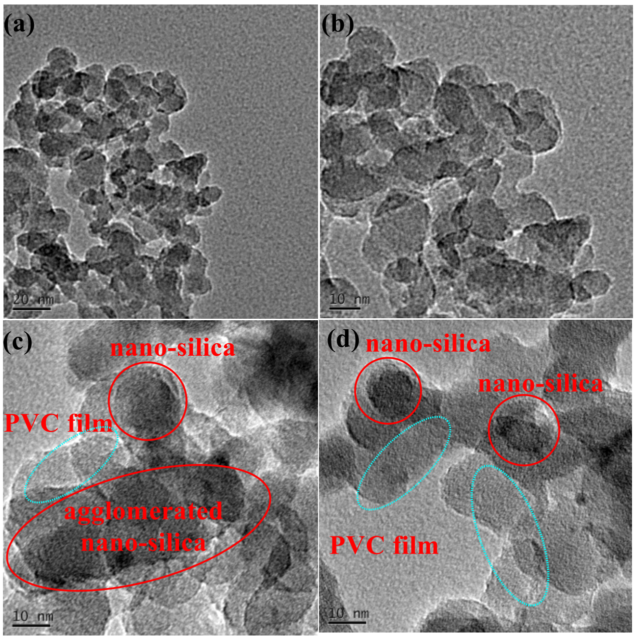

Figure 5. HRTEM images NS@PVC-EDA-SO_3H catalyst.

STEM-EDS: The distribution and content of this catalyst's surface elements were further investigated using high resolution scanning transmission electron microscopy (HRSTEM) equipped with a high-angle annular dark field (HAADF) and energy-dispersive spectroscopy (EDS) detectors. As shown in Figure 6 (a, c-e), an overlay and single elemental mappings for the surface Si and C elements of NS@PVC-EDA-SO_3H show relatively uniform distributions in the regions marked with the green circles but are an obvious inhomogeneities in the unmarked other regions, which can well correspond to its HRTEM images. Notably, the distributions of N and especially S elements in the two mappings (Figure 6f, h) are very similar to that of C element, supporting that EDA and LHS can be homogeneously grafted on the PVC in successive. The Cl element presents an obviously sparse distribution in its mapping (Figure 6g), further supporting that most C-Cl bonds of PVC have been substituted by C-N bonds *via* N-alkylation. Furthermore, the real content of loading PVC measured via high temperature combustion method approximately accounts for 72.3% of the loading PVC (31.5%, calculated according to carbon element measured via energy-dispersive spectroscopy, which indicated that PVC covers successfully the surface of the NS. Notably, the amount of SO_3H groups on NS@PVC-EDA-SO_3H calculated from EDS analysis of Figure 6 (b) is 1.12 mmol•g^{-1}, which closes to the acid density measured via chemical analysis (1.26 mmol•g^{-1}), indicating that most of the -SO_3H groups are exposed on the surface of the catalyst, only a small amount of SO_3H groups are enclosed in the dense layer of the NS@PVC-EDA-SO_3H.

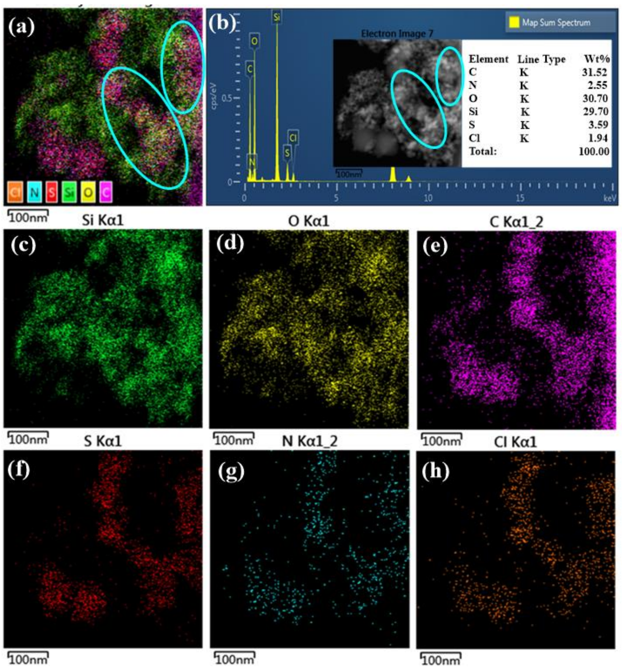

Figure 6. Elemental mappings and energy-dispersive spectroscopy analyses of NS@PVC-EDA-SO_3H catalyst.

3.2 Catalytic performance of NS@PVC-EDA-SO_3H

Effects of average particle size of NS support: The effect of average particle size of NS support on the acid density and hydroxyalkylation performance of NS@PVC-EDA-SO_3H catalyst was studied and the results are listed in Table 2. It can be seen from Table 2 that the acid density of catalyst, formaldehyde conversion and BPF selectivity increase with decreasing silica's average particle size from 60 to 0.02 μm. This is probably because the catalyst prepared using the small size of NS not only has higher sulfamic acid sites but also its short pore channels are conducive to improve the exposure of the acid sites and accelerate the diffusion of the reactants to the acid sites, thus leading to it showing excellent formaldehyde conversion activity (98.1%) and BPF selectivity (92.2%).

Effect of activation temperature of NS: The effect of NS's activation temperature on the acid density and hydroxyalkylation performance of NS@PVC-EDA-SO_3H catalyst was studied and the results are shown in Figure 7. The results indicate that the acid density of the catalyst and the formaldehyde conversion over it gradually increase with elevating the activation temperature, respectively achieving the highest 1.26 mmol·g^{-1} and 99.6% at 200°C. After that, its acid density and the conversion are gradually reduced to 0.83 mmol·g^{-1} and 74.6%, accompanied by BPF selectivity decreased by 16%. The above effects of the activated temperature likely originate from its regulation on the surface properties of NS, the low activated temperature hardly completely remove the physically absorbed water on NS surface[38,39],while the high activated temperature significantly reduces the silanols on NS surface via dehydration[40], a large amount of adsorbed water or low density of silanols may reduce the loading efficiency of PVC on the NS carrier, thus leading to a significant decrease in the acid sites and hydroxyalkylated activity of catalyst. Here, 200°C was selected as the preferred activation temperature of NS for the preparation of an excellent catalyst.

Table 2. Effects of NS's average particle size on catalyst performance of NS@PVC-EDA-SO_3H catalyst [a]

NS's average particle size (μm)	Acid density (mmol·g^{-1})	HCHO conv. (%)	BPF sel. (%)	BPF isomer distribution (%)		
				4,4'-BPF	2,4'-BPF	2,2'-BPF
60	0.52	77.9	73.6	55.2	33.4	11.4
20	0.69	86.9	88.2	39.6	41.8	18.6
0.02	0.81	98.1	92.2	34.7	44.6	20.7

[a] Reaction conditions: silica average particle size, 60 μm, 20 μm, 0.02 μm; Activation conditions, 200°C, 5 h; wt.%= *m(PVC)/m(silica)*, 20%. 10 mmol formaldehyde, mole ratio of phenol/formaldehyde, 20; Catalyst concentration, 3.0 wt.%; Reaction time, 1 h; Reaction temperature, 70°C.

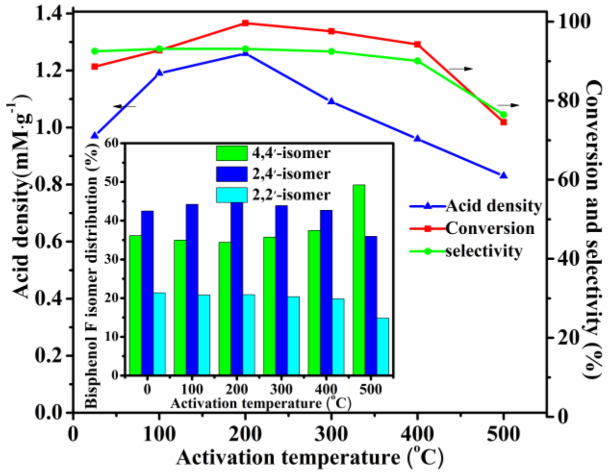

Figure 7. Effect of activation temperature on the performance of NS@PVC-EDA-SO_3H catalyst [a]

[a] Reaction conditions: silica average particle size, 0.02 um; Activation conditions, 100~500°C, 5 h; wt.% = *m(PVC)/m(silica)*, 40%. 10 mmol formaldehyde, mole ratio of phenol/formaldehyde, 20; Catalyst concentration, 3.0 wt.%; Reaction time, 1 h; Reaction temperature, 70°C;

Effect of PVC loading: Considering the close relationship between PVC loading and acid sites on the surface of catalyst, a series of NS@PVC-EDA-SO_3H catalysts were prepared using 10 to 50 wt.% PVC dosages and their catalysis performances were evaluated by the hydroxyalkylation of phenol with formaldehyde to BPF. As shown in Figure 8. The acid density increases from 0.61 to 1.26 mmol·g-1 and the formaldehyde conversion increases from 82.1 to 99.4%, with PVC loading consequently increasing from 10 to 40%. The reason for this result may be the amount of amino groups increases with the increase in PVC loading, and the larger PVC loading on the surface of silica, the more amino groups are grafted on the carbon chain, so a large number of SO_3H groups can be obtained after chlorosulfonation. However, the acid density, formaldehyde conversion and selectivity to BPF shows no significant increase upon further increases in PVC loading. Therefore, a solid acid catalyst with high catalytic performance was obtained when the PVC loading is 40 wt.%.

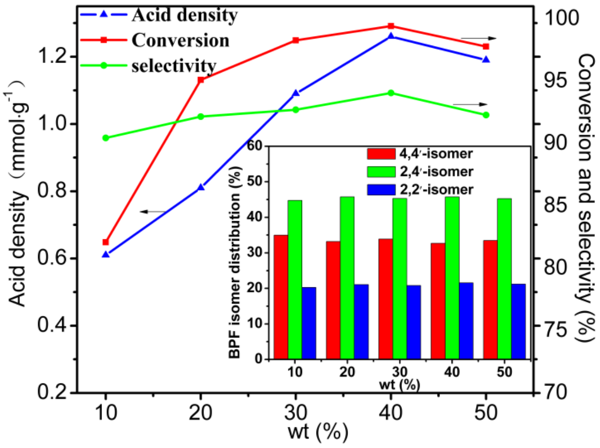

Figure 8. Effect of PVC loading on catalyst performance of NS@PVC-EDA-SO_3H catalyst [a]

[a] Reaction conditions: silica average particle size, 0.02 um; Activation conditions, 200°C, 5 h; wt.% = *m(PVC)/m(silica)*, 10~50%. 10 mmol formaldehyde, mole ratio of phenol/formaldehyde, 20; Catalyst concentration, 3.0 wt.%; Reaction time, 1 h; Reaction temperature, 70°C.

Effects of reaction temperature: The influence of reaction temperature on hydroxyalkylation was examined under catalysis of the best NS@PVC-EDA-SO_3H. As shown in Figure 9, this catalyst shows a good low temperature activity and can provide 78.8% formaldehyde conversion and 81.4 % BPF selectivity at 45°C. As reaction temperature is elevated to 70°C, the conversion and selectivity continuously and remarkably increase to 99.6 and 93.9%, respectively. After that, the enhanced effect of temperature on hydroxyalkylation is almost invalid. The distribution of three isomers in bisphenol F products varies obviously in the range of 45–60°C and the selectivity for 2,4'- and 2,2'-isomers is improved with elevating the temperature, further supporting that 2-hydroxybenzyl alcohol has a lower activity than 4-hydroxybenzyl alcohol and needs a higher temperature to accelerate its conversion to such two isomers.

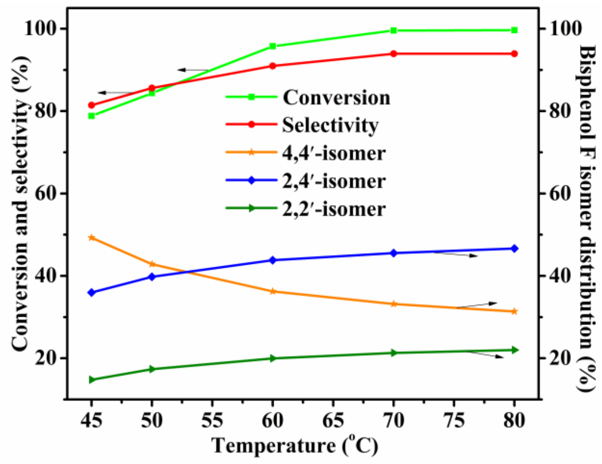

Figure 9. Effect of reaction temperature on the hydroxyalkylation of phenol with formaldehyde [a]

[a] Reaction conditions: 10 mmol formaldehyde, mole ratio of phenol/formaldehyde, 20; Catalyst concentration, 0.25% mol; Reaction temperature, 45-70^{o}C; Reaction time, 1 h.

Effects of catalyst concentration: The effect of catalyst concentration on hydroxyalkylation was also checked using the optimal NS@PVC-EDA-SO_3H as a catalyst. As shown in Figure 10. The activity and selectivity of catalyst continuously and markedly increase with a gradual increase of its concentration, which can achieve 97.5% formaldehyde conversion and 93.0% BPF selectivity at 0.1 mol % catalyst concentration. Upon further increase in catalyst concentration, the formaldehyde conversion and selectivity to BPF only show a minor change. Thus, 0.1% mol is selected as the suitable catalyst concentration. Notably, the distribution of three isomers in BPF products is influenced by catalyst concentration, as the concentration of catalyst is enhanced from 0.025 to 0.050% mol, 2,4'- and 2,2'-isomers increase from 41.2 to 45.8% and from 17.2 to 21.6%, respectively, along a significant decrease in 4,4'-isomer from 41.6 to 32.7%. This is perhaps because an increase in the acid amount relied on catalyst concentration can accelerate the conversion of the intermediate 2-hydroxybenzyl alcohol to 2,4'- and 2,2'-isomers.

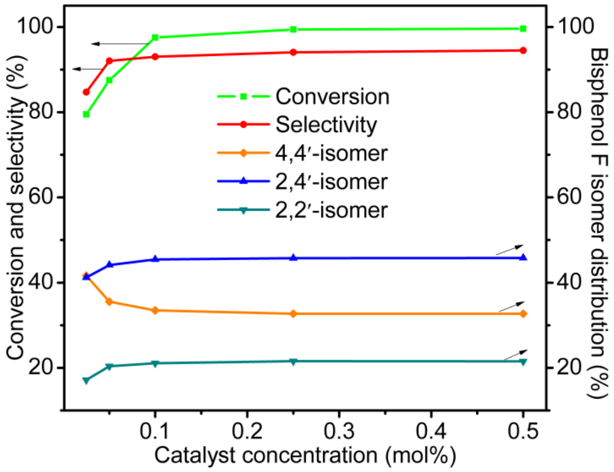

Figure 10. Effect of catalyst concentration on the hydroxyalkylation of phenol with formaldehyde [a]

[a]Reaction conditions: 10 mmol formaldehyde, mole ratio of phenol/formaldehyde, 20; Catalyst concentration, 0.025~0.500% mol; Reaction time, 1 h; Reaction temperature, 70^{o}C.

Effects of reaction time: The influence of reaction time on hydroxyalkylation was examined under catalysis of the best NS@PVC-EDA-SO_3H and the results shown in Figure 11. Such catalyst exhibits an outstanding acceleration effect on hydroxyalkylation, which can afford 38.5% formaldehyde conversion and 82.3% BPF selectivity at 5 min. When the time is prolonged from 5 to 60 min, the conversion and selectivity further increase to 98.3 and 94.0%, respectively. At the same, the 2,4'- and 2,2'- BPF isomers gradually increase from 38.1% to 45.7% and 16.9% to 21.6%, respectively. This may be because the intermediate 4-hydroxybenzyl alcohol is rapidly and mainly converted to 4,4'-isomer in the early reaction period, while the rate of another intermediate 2-hydroxybenzyl alcohol being converted to 2,4'- and 2,2'-isomers is not so fast. Hence the amount of 4,4'-isomer is dominant in the initial period. As the reaction proceeds, the intermediate 2-hydroxybenzyl alcohol could be converted to 2,4'- and 2,2'-isomers more quickly. So, the selectivity of 2,4'- and 2,2'-isomers increases obviously, whereas the distribution of 4,4'-isomer decreased relatively. Therefore, the optimal reaction time is 1 h.

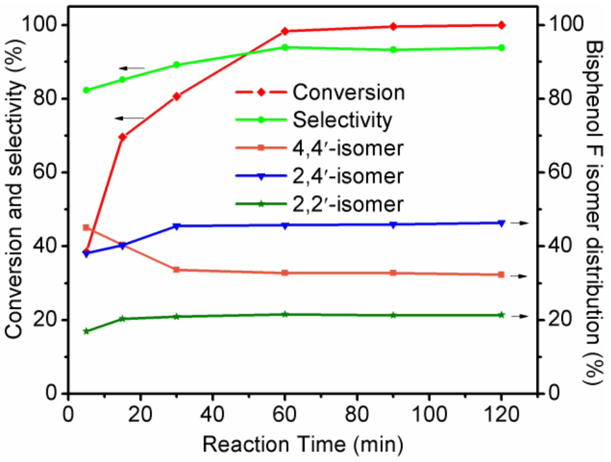

Figure 11. Effect of reaction time on the hydroxyalkylation of phenol with formaldehyde [a]

[a] Reaction conditions:10 mmol formaldehyde, mole ratio of phenol/formaldehyde, 20; Catalyst concentration, 0.1% mol; Reaction time, 5~120 min; Reaction temperature, 70^{o}C.

Compared with existing homogeneous and heterogeneous catalysts: The catalytic hydroxyalkylation performance of NS@PVC-EDA-SO_3H was compared to those of two reference catalysts (the existing concentrated sulfuric acid (H_2SO_4) and sulfonic acid resin) and the results are shown in Figure 12, NS@PVC-EDA-SO_3H catalyst exhibits an outstanding hydroxyalkylation activity, which can achieve 92.9% formaldehyde conversion and 93.1% BPF selectivity. While homogeneous H_2SO_4 and heterogeneous sulfonated resin catalysts only provide 53.4 and 12.9 % formaldehyde conversions under the same reaction conditions, respectively. Furthermore, its BPF selectivity (93.1%) is also higher than those of H_2SO_4 (89.9%) and especially sulfonated resin (74.7%). As a heterogeneous solid acid catalyst, NS@PVC-EDA-SO_3H has an absolute advantage over concentrated sulfuric acid in the reusability. With a higher dispersibility, NS@PVC-EDA-SO_3H shows a better catalytic activity than sulfonic acid resin. These compared data support that NS@PVC-EDA-SO_3H, as a newly constructed solid acid catalyst, has an overwhelming advantage in hydroxyalkylation performance compared to the two existing reference catalysts, expecting that it has extensive application prospects in acid catalysis reactions, especially including hydroxyalkylations.

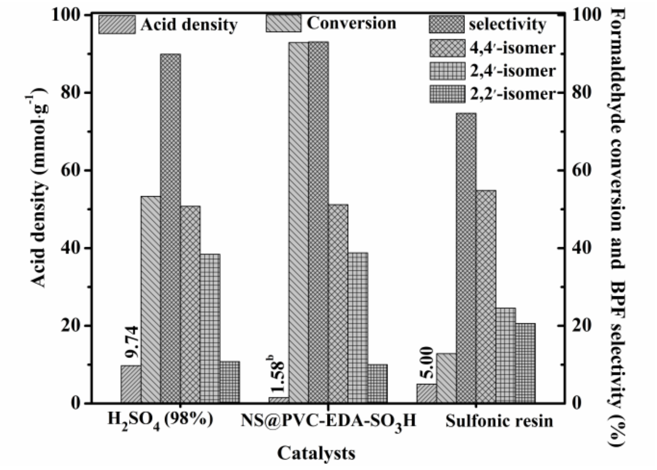

Figure 12. The catalytic performance of different catalysts in the synthesis of BPF [a]

[a] Reaction conditions:10 mmol formaldehyde, mole ratio of phenol/formaldehyde, 20; Catalyst concentration, 0.1% mol (10 mg concentrated sulfuric acid, 60 mg NS@PVC-EDA-SO_3H catalyst, 20 mg sulfonic acid resin); Reaction temperature, 60°C; Reaction time, 1 h. [b] Re-prepared catalyst.

Comparison of catalytic activity of NS, NS@PVC, NS@PVC-EDA, NS@PVC-SO_3H and PVC-EDA-SO_3H catalyst: The catalytic hydroxyalkylation performance of NS@PVC-EDA-SO_3H was compared to NS, NS@PVC, NS@PVC-EDA, NS@PVC-SO_3H and PVC-EDA-SO_3H catalysts and the results are shown in Figure 13. It can be seen that NS@PVC-EDA-SO_3H catalyst exhibits an outstanding superiority in catalytic activity compared to those catalysts, which can achieve 99.6% formaldehyde conversion and 93.3% BPF selectivity. While NS, NS@PVC, NS@PVC-EDA catalysts show a poor hydroxyalkylation activity, which obtains a extremely low formaldehyde conversion. It is worth mentioning that NS@PVC-SO_3H and PVC-EDA-SO_3H catalysts also has a remarkable catalytic activity for hydroxyalkylation, provide 77.4 and 85.9 % formaldehyde conversions under the same reaction conditions, respectively. However, NS@PVC-EDA-SO_3H has a greater advantage in hydroxyalkylation. This may be due to the fact that the NS@PVC-EDA-SO_3H catalyst has a mesoporous to macroporous structure that can accelerate the diffusion and conversion of substrates.

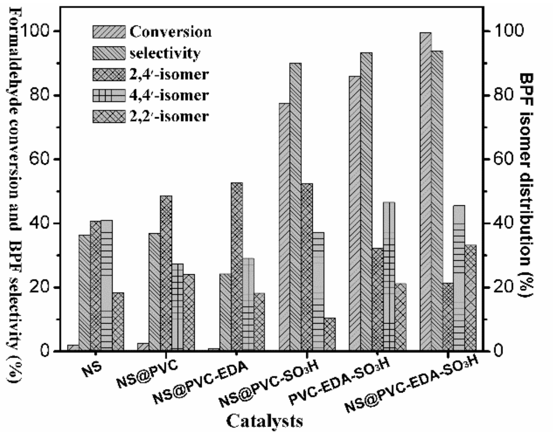

Figure 13. Comparison of catalytic activity of NS, NS@PVC, NS@PVC-EDA, NS@PVC-SO_3H and PVC-EDA-SO_3H catalyst [a]

[a] Reaction conditions:10 mmol formaldehyde, mole ratio of phenol/formaldehyde, 20; Catalyst concentration, 0.1% mol; Reaction time, 1 h; Reaction temperature, 70°C.

Reusability of the catalyst: Finally, the stability of NS@PVC-EDA-SO_3H was tested by performing a recycle experiment and the testing results are presented in Figure 14. The performance of the catalyst shows no significant reduction even after nine successive runs, still achieving 97.6% formaldehyde conversion and 93.5% BPF selectivity, Furthermore, the distribution of the isomers in BPF products only varies slightly in all the recycle experiments. Thus, NS@PVC-EDA-SO_3H is considered to be an excellent and stable recyclable solid acid catalyst for the current hydroxyalkylation.

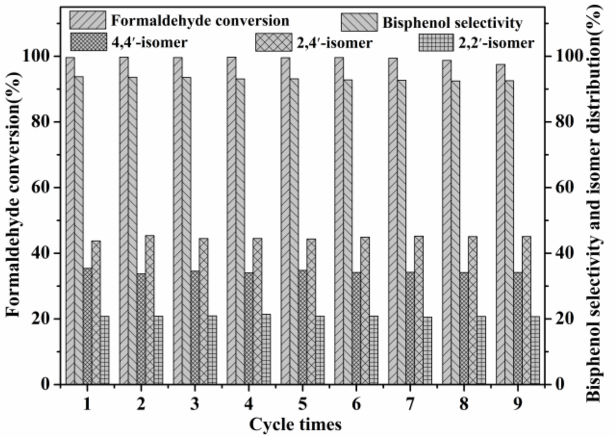

Figure 14. Reusability of catalyst study [a]

[a] Reaction conditions:10 mmol formaldehyde, mole ratio of phenol/formaldehyde, 20; Catalyst concentration, 0.25% mol; Reaction temperature, 70°C; Reaction time, 1 h.

The plausible mechanism for formation of bisphenol F: A plausible mechanism of condensation of phenol and formaldehyde to BPF is presented in scheme 2. A carbocation CH_2OH^+ is formed by protonation of formaldehyde with H^+ released by -SO_3H in NS@PVC-EDA-SO_3H. An electrophilic substitution reaction occurs on phenol with the formation of two intermediates I(a) and I(b) as the first step, then the short-lived intermediates I (b) and I (a) deprotonates fast to form II (a) 2-hydroxybenzylalcohol and II (b) 4-hydroxybenzyl The protonation of alcohol II (a) and II (b) initially produced form the carbocation III (a) and III (b) respectively. A complexation of the electrophile carbocation III (a) and III (b) with the π electron system of another phenol molecule generates three intermediates IV(a), IV(b) and IV(c): these unstable intermediates then eliminate a proton, resulting in final formation of BPF (V(a) 2,2'-BPF, V(b) 2,4'-BPF and V(c) 4,4'-BPF).

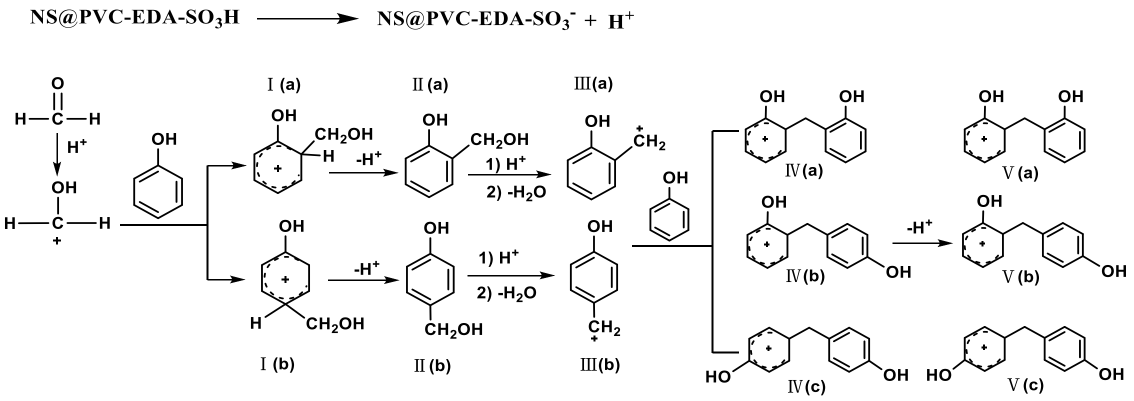

Scheme 2. Plausible mechanism of condensation of phenol and formaldehyde to BPF

4. Conclusion

In summary, NS@PVC-EDA-SO_3H catalyst with richer short mesoporous to macroporous channels has been successfully synthesized *via* multi-steps treatment processes and this newly constructed solid acid catalyst offers several promising advantages in the hydroxyalkylation of phenol with formaldehyde to BPF, including excellent catalytic activity and selectivity, as well as easy recovery and good recyclability. With such kind of renewable solid acid in hand, we are interested in further exploring its potential applications to other important acid-catalyzed reactions in industry, such as esterification, alkylation, hydrolysis and so on .

Acknowledgement

This research is financially supported by the National Natural Science Foundation of China (Nos. 21546010, 21576078, 21676079, 21606082, 21776068), the National & Local United Innovation Platform (No. 20123098), and the Natural Science Foundation of Hunan Province (Grant No. 2016JJ2081). Hunan 2011 Collaborative Innovation Center of Chemical Engineering & Technology with Environmental Benignity and Effective Resource Utilization.

References

1. X. Zhang, Q. He, H. Gu, H. A. Colorado, S. Wei and Z. Guo, ACS appl. mat. Interfaces **2013**, 5, 898-910.
2. Q. Wang, Z. M. Wu, Y. Li, Y. Tan, N. Liu and Y. Liu, Rsc Adv. **2014**, 4, 33466-33473.
3. M. Okihama, J. Kunitake, Jpn. Kokai Tokkyo Koho. JP 08198790 (**1996**)
4. M. Okihama, J. Kunitake, Jpn. Kokai Tokkyo Koho. JP 08268943 (**1996**)
5. M. Okihama, J. Kunitake, Jpn. Kokai Tokkyo Koho. JP 09067287 (**1997**).
6. Y. Zuo, Y. Zhang, Y. Fu, Chemcatchem **2014**, 6, 753-757.
7. J. Chen, J. Chen, X. Zhang, J. Gao and Q. Yang, Appl. Catal. A Gen. **2016**, 516, 1-8.
8. F. K. Esfahani, D. Zareyee, R. Yousefi, Chemcatchem **2015**, 6, 3333-3337.
9. X. Wu, Y. Liu, L. Ran, L. Wang, Y. Lu and X. Xia, J. Colloid Interface Sci. **2016**, 481, 75-81.
10. S. K. Jana, H. Takahashi, M. Nakamura, M. Kaneko, R. Nishida, H. Shimizu, T. Kugita and S. Namba, Appl. Catal. A Gen. **2003**, 245, 33-41.
11. X. Wu, X. Xia, R. Liu and Y. Chen, Rsc Adv. **2016**, 6, 34625-34632.
12. S. K. Jana, T. Okamoto, T. Kugita and S. Namba, Appl. Catal. A Gen. **2005**, 288, 80-85.
13. M. Chen, J. Yan, Y. Tan, Y. Li, Z. Wu, L. Pan and Y. Liu, Ind. Eng. Chem. Res. **2015**, 266, 245-250.
14. S. K. Jana, T. Kugita and S. Namba, Appl. Catal. A Gen. **2004**, 266, 245-250.
15. Y. Wei, Y. Li, Y. Tan, Z. Wu, L. Pan and Y. Liu, Chem. Eng. J. **2016**, 298, 271-280.
16. A. C. Garade, V. S. Kshirsagar and C. V. Rode, Appl. Catal. A Gen. **2009**, 354,176-182.
17. S.Y. Chen, C.Y. Tang, W.T. Chuang, J.J. Lee, Y.L. Tsai, J.C.C. Chan, C.Y. Lin, S. Cheng, Chem. Mater. **2008**, 20, 3906–3916.
18. S.Y. Chen, Y.T. Chen, J.J. Leec, S. f. Cheng, , J. Mater. Chem. **2011**, 21, 5693–5703.
19. S.Y. Chen, T. Yokoi, C.Y. Tang, L.Y. Jang, T. Tatsumi, C.C. Jerry, S. Cheng, Green Chem. **2011**, 13, 2920–2930.
20. E.A. Sujandi, S.E. Prasetyanto, Park, Appl. Catal. A Gen. **2008**, 350, 244–251.
21. K. Akli, K. Supadi and I. G. Wenten, J. Membr. Sci. Res. **2014**, 482, 258-265.
22. X. N. Zhao, H. C. Hu, F. J. Zhang and Z. H. Zhang, Appl. Catal. A Gen. **2014**, 482, 258-265.
23. F. Reche, M. Garrigós, A. Sánchez and A. Jiménez, J. Chromatogr. A **2000**, 89, 651-59.
24. H. C. Loh, K. W. Chong, M. Ahamad, Anal. Lett. **2007**, 40, 281-293.
25. Z. Chao, Z. H. Fu, Y. C. Liu, B. H. Dai, Y. H. Zou, X. L. Gong, Y. L. Wang, X. L. Deng, H. T. Wu and Q. O. Xu, Green Chem. **2012**, 14, 1928-1934.
26. Y. Turhan, M. Do, M. Alkan, Adv. Polym. Technol. **2013**, 32, 65–82.
27. Y. Turhan, M. Doğan and M. Alkan, Ind. Eng. Chem. Res. **2010**, 49, 1503-1513.
28. M. Parveen, S. Azaz, F. Ahmad, et al., Catal. Lett. 2016, 146, 1687-1705.
29. M. Sheykhan, M. Leila, A. Ebrahimi, et al., J. Mol. Catal. A Chem., **2011**, 335, 253-261.
30. K. Niknam, A. Jamali, M. Tajaddod, et al., Chin. J. Catal., **2012**, 33, 1312-1317.
31. S. Tarannum and Z. N. Siddiqui, Monatsh. Chem., **2017**, 148, 1-14.
32. F. A. Al-Sagheer and Z. Ahmad, J. Sol-Gel Sci. Technol. **2011**, 61, 229-235.
33. D. Q. Vu, W. J. Koros, S. J. Miller. J. Membr. Sci., **2003**, 211, 311-334.
34. M. P. Chenar, M. Mohagheghian, M. Sadeghi, Korean J. Chem. Eng. **2014**, 31, 2041-2050.
35. S. Rostamnia and E. Doustkhah, J. Mol. Catal. A Chem. **2015**, 411, 317-324.
36. S. Maheswaran, B. Bhuvaneshwari, G. S. Palani, N. R. Iyer and S. Kalaiselvam, J. Sol-Gel Sci. Technol. **2012**, 61, 229-235.
37. W. E. Mahmoud, Eur. Polym. J. **2011**, 47, 1534-1540.

38. A. Zhu, A. Cai, Z. Jie, H. Jia, J. Wang, J. Appl. Pol. Sci. **2010**, 108, 2189-2196.
39. A. Zhu, A. Cai, W. Zhou, Z. Shi, *Appl. Surf. Sci.* **2008**, 254, 3745-3752.
40. T. Garoff, M. Väänänen, A. Root, M. Stålhammar, K. Pesonen. Eur. Pol. J. **2007**, 43, 5055-5064.